Magnetic and transport properties in $CoSr_2Y_{1-x}Ca_xCu_2O_7$ ($x=0-0.4$)

X. G. Luo, X. H. Chen,* X. Liu, R. T. Wang, Y. M. Xiong, C. H. Wang, and G. Y. Wang
Structure Research Laboratory and Department of Physics, University of Science and Technology of China, Hefei, Anhui, 230026, People's Republic of China

X. G. Qiu
State Key Laboratory of Superconductivity, Institute of Physics, Chinese Academy of Sciences, Beijing 10080, People's Republic of China
(Received 2 January 2004; revised manuscript received 28 April 2004; published 31 August 2004)

Magnetic and transport properties of $CoSr_2Y_{1-x}Ca_xCu_2O_7$ ($x=0-0.4$) system have been investigated. A broad maximum in the $M(T)$ curve, indicative of low-dimensional antiferromagnetic ordering originated from $CoO_{1+\delta}$ layers, is observed in the Ca-free sample. With increasing as Ca doping level up to 0.2, the $M(T)$ curve remains almost unchanged, while resistivity is reduced by three orders. A higher Ca doping level leads to a drastic change of magnetic properties. In comparison with the samples with $x=0.0-0.2$, the temperature corresponding to the maximum of $M(T)$ is much lower for the sample $x=0.3$. The sample $x=0.4$ shows a small kink instead of a broad maximum and a weak ferromagnetic feature. The electrical transport behavior is found to be closely related to magnetic properties for the sample $x=0.2$, 0.25, 0.3, 0.4. It suggests that $CoO_{1+\delta}$ layers are involved in charge transport, in addition to conducting CuO_2 planes to interpret the correlation between magnetism and charge transport. X-ray photoelectron spectroscopy studies give additional evidence of the the transfer of the holes into the $CoO_{1+\delta}$ charge reservoir.

DOI: 10.1103/PhysRevB.70.054520 PACS number(s): 74.72.Bk, 74.25.Ha, 74.25.Fy

I. INTRODUCTION

Charge transport and high temperature superconductivity (HTSC) is believed to reside in the CuO_2 planes of all known HTSC cuprates,[1] except that $CuO_{1+\delta}$ chains have been reported to participate in the *b*-axis transport of $YBa_2Cu_3O_{7-\delta}$.[2] In $YBa_2Cu_3O_{7-\delta}$ (also denoted as $CuYBa_2Cu_2O_{7-\delta}$, Cu1212) there are two different Cu sites, namely Cu(2) and Cu(1). Cu(2) resides in superconducting CuO_2 planes and Cu(1) in $CuO_{1+\delta}$ chains. Any breach of integral CuO_2 stacks, even at macroscopic level, affects superconductivity drastically. The $CuO_{1+\delta}$ chain acts as a charge reservoir and provides the mobile carriers to superconducting CuO_2 planes.

Some attempts have been performed successfully for complete replacement of $CuO_{1+\delta}$ by other metal elements. $MSr_2YCu_2O_{7+\delta}$ (M-1212, M=Pb, Ru, Nb, Al, Hg, Fe, Ga, Ta, etc.)[3–8] have attracted extensive attention in the past. Some of them have been made superconducting, such as Nb1212, Hg1212, Ru1212, Tl1212, Ga1212, and Fe1212,[6–8] and some others, like Ta1212, remain nonsuperconducting. Another example, Co1212, kept nonsuperconducting since it was synthesized first in 1989,[3] until very recently, Morita *et al.* made it superconducting (SC) by annealing Ca-doped Co1212 in ultrahigh O_2 pressure (5 Gpa).[9] However, the reason why the system is not SC before ultrahigh pressure treatment and it becomes SC after ultrahigh pressure treatment, still remains unknown.

Up to now, the research for Co1212 has been focused on its structure and magnetic properties.[10–12] The structure of Co1212 is derived from $CuBa_2YCu_2O_{7-\delta}$ (Cu1212), by completely substituting divalent Cu(1) in the $CuO_{1+\delta}$ charge reservoir of Cu1212 with a trivalent Co ion. In Cu1212 the charge reservoir Cu atom with surrounding oxygen atoms forms a square CuO_4 polyhedron. However, the CoO_4 tetrahedral coordination polyhedron has been reported in Co1212.[10] Ga1212[4] and Al-1212[13,14] have also been reported to have the tetrahedral polyhedron. Such CoO_4 tetrahedra forms a zigzag chain running diagonally relative to the pervoskite base. A regular alternation of two zigzag chains, which are mirror images of each other, forms an orthorhombic superstructure.[15] Unlike CuO_4 square chains in Cu1212, which are very easy to lose or obtain oxygen, the CoO_4 tetrahedral chains in Co1212 are reported to be a rigid configuration in terms of oxygen content.[16] In Co1212, all of the Co ions reside on the Cu(1) sites.[10] With Y^{3+} substituted by Co^{2+}, however, Co and Cu will intermixed partly. The $M(T)$ curve of Co1212 exhibits a broad maximum, indicative of a low-dimensional magnetic ordering, which was thought to originating from Co^{3+} spin.[11] With no doubt, studies on the function of CoO_4 tetrahedra certainly give very useful information to settle the forenamed question. In the present report, we investigated the magnetic and electrical properties on Ca substituted Co1212 from Ca content 0.0–0.4. It is found that with increasing Ca doping level, electrical transport properties become related to magnetic structure closely. Magnetic properties and their correlation with charge transport suggest that slightly partial holes induced by Ca doping reside on the $CoO_{1+\delta}$ layers and these holes influence the magnetic and charge transport properties dramatically. In addition, these holes cause $CoO_{1+\delta}$ to participate in bulk electrical transport. X-ray photoelectron spectroscopy (XPS) studies indicate that for high Ca doping level, the valence of Co increases comparing to the low doping level and thus confirm that holes enter into the charge reservoir.

II. EXPERIMENT

A series of samples with compound of $CoSr_2Y_{1-x}Ca_xCu_2O_{7+\delta}$ ($x=0.0-0.4$) were synthesized

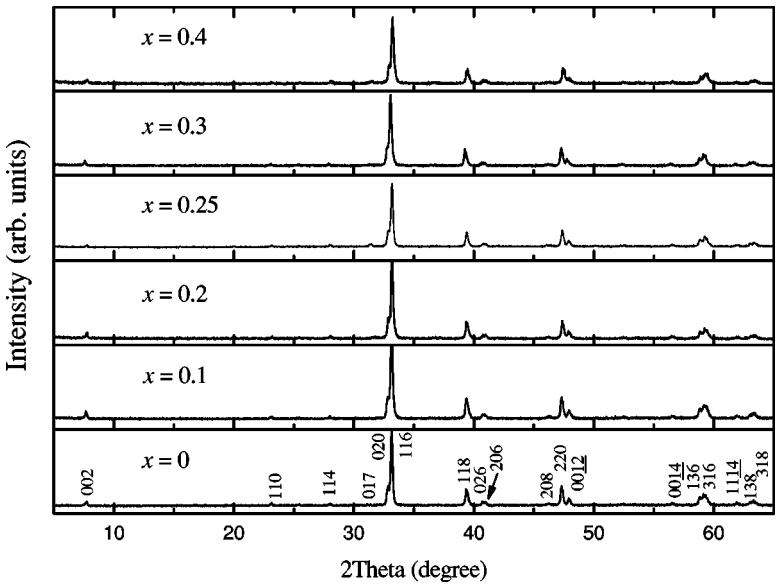

FIG. 1. XRD patterns for the as-synthesized samples of $CoSr_2Y_{1-x}Ca_xCu_2O_{7+\delta}$ ($x=0.0-0.4$).

through a solid-state reaction route. Co_2O_3, $SrCO_3$, Y_2O_3, $CaCO_3$, and CuO, as the starting materials, were mixed in nominal composition and heated for 24 h at 950 °C and another 24 h at 1000 °C with intermediate grinding. Finally, the products were pelletized and sintered at 1010 °C for 24 h. The phase purity was checked for each sample with powder x-ray diffraction (XRD). Magnetization measurements were performed on each sample with a superconducting quantum interference device (SQUID) magnetometer in field cooling mode. For the samples $x=0.25$ and 0.4, additional zero-field cooling (ZFC) magnetization were performed. Resistance measurements were performed using an ac four-probe method with an ac bridge resistance bridge system (Linear Research, Inc.; LR-700P). All samples for magnetization and resistance measurements have been annealed under 195 atm oxygen atmosphere at 500 °C for 24 h. It should be pointed out that the sample annealed under 195 atm and ambient pressure oxygen atmosphere shows almost the same behavior in charge transport and magnetism. These results further confirm that the oxygen content in Co1212 cannot change easily. The XPS spectra were collected with an ESCALAB MK II electron spectrometer using Mg Kα radiation as an excitation source ($h\nu=1253.6$ eV). Binding energy was calibrated with a reference of surface contaminated C 1 s ($E_b=284.6$ eV). The basic vacuum was about 1×10^{-9} mbar.

III. RESULTS AND DISCUSSION

XRD patterns for as-synthesized (AS) samples with various Ca content, x, are shown in Fig. 1. No any visible impurity peak in XRD patterns is observed for all samples. All the peaks can be indexed using the space group *Ima*2.[10] It demonstrates all the samples are single-phase materials and have the orthorhombic structure. The lattice parameters determined from the XRD patterns with the Rietveld method in the GSAS program are plotted against x in Fig. 2. (note that the c axis here as referred to the layer piling direction as typically employed for the structures of high-T_c superconductors, and the a axis is along the $CoO_{1+\delta}$ chain.) With increasing Ca content x, the lattice parameter of the a axis slightly increases, while the b axis shrinks a little. An in-

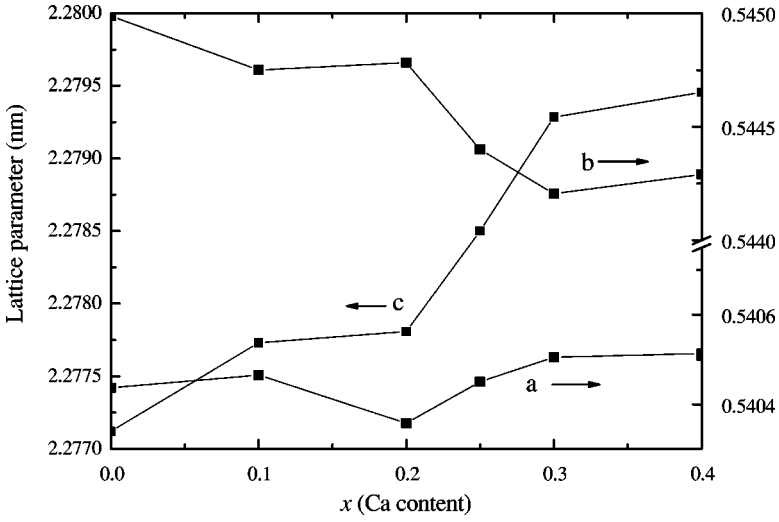

FIG. 2. Lattice parameters for the as-synthesized samples of $CoSr_2Y_{1-x}Ca_xCu_2O_{7+\delta}$.

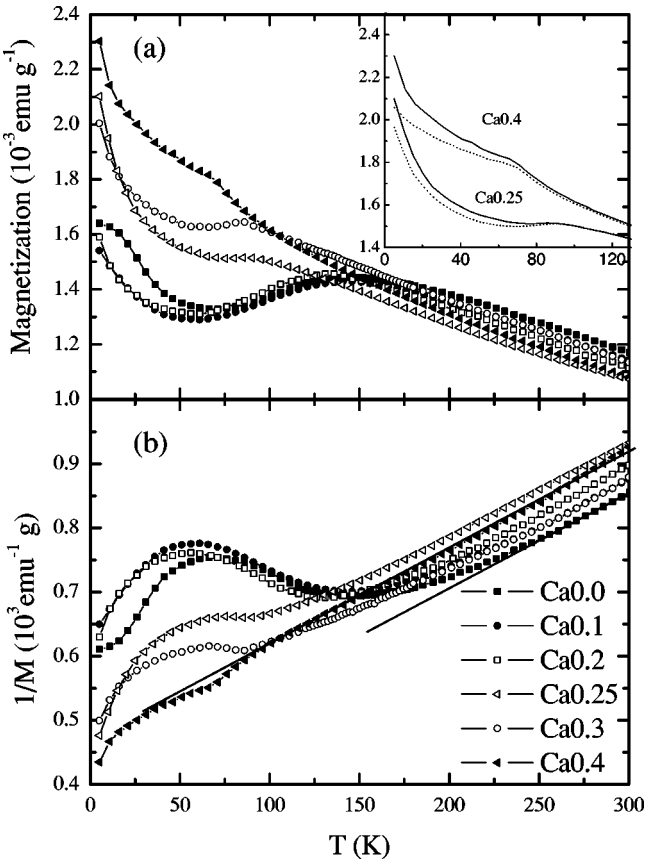

FIG. 3. (a) The temperature dependence of magnetization measured for the annealed $CoSr_2Y_{1-x}Ca_xCu_2O_{7+\delta}$ samples in field-cooled process at the field of 100 Oe. Inset: ZFC (dashed line) and FC (solid line) data at the field of 100 Oe plotted against the temperature for the samples $x=0.25$ and 0.4. (b) The temperature dependence of inverse magnetization for the sample $x=0.0-0.4$.

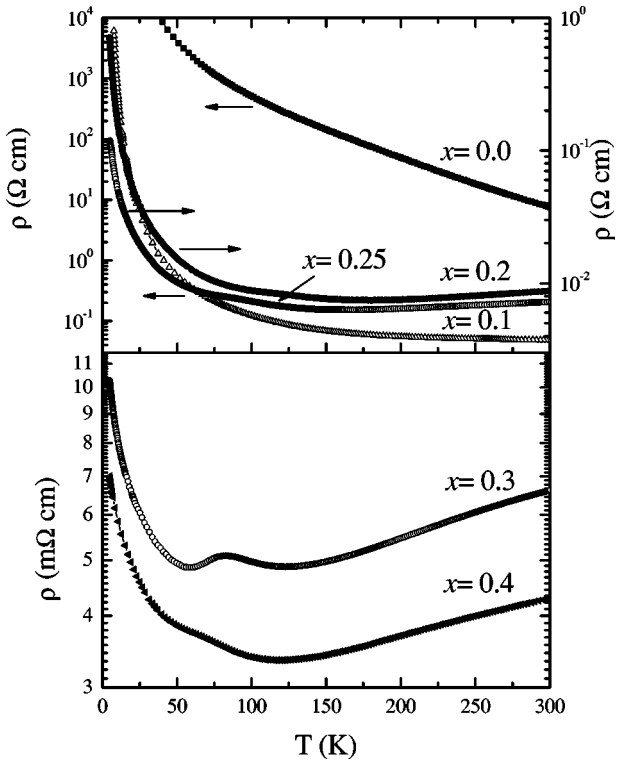

FIG. 4. The resistivity as a function of temperature for the annealed $CoSr_2Y_{1-x}Ca_xCu_2O_{7+\delta}$ samples.

crease of c axis parameter with x demonstrates that the doped Ca ions have entered into Y sites instead of Sr sites. The reason is that the radius of Ca^{2+} is larger than Y^{3+}, but less than Sr^{2+}, thus substitution of Sr^{2+} by Ca^{2+} should cause a shrinkage of the c axis. It has been reported that the oxygen content in Ca-doped Co1212 almost remains constant,[9] thus replacing partial trivalent Y ion by divalent Ca ion results in excess holes to system.

Figure 3 shows the temperature dependence of the dc magnetization (M) of annealed samples $x=0.0-0.4$. The magnetization of Ca-free sample shows a broad maximum around 145 K and then a shallow downturn followed by an upturn with decreasing temperature, which agree well with the previous reports.[11,12] The analogous field-cooled (FC) $M(T)$ curve has been observed in $Sr_2CoCuS_2O_2$,[17] Sr_2CuMnO_3S,[18] Sr_2MnO_3Cl, and $Sr_4Mn_3O_{8-y}Cl_2$,[19] in which the broad maximum was thought to be indicative of a low-dimensional magnetic feature.[20] The inverse of magnetization displays an upturn deviation from linear behavior with decreasing temperature, indicative of antiferromagnetic ordering. Considering the three-dimensional (3D) magnetic character of a high-T_c system, the low-dimensional antiferromagnetic feature most likely originates from the Co-O layers instead of Cu-O planes. In addition, magnetization remains almost unchanged for $x=0.1$ and 0.2 except for a little lowering of the temperature of maximum, indicating that the holes induced by Ca doping enter into the Cu-O plane. The drastic drop of resistivity with x increasing from 0.0 to 0.2 confirms this speculation, which will be discussed later. As shown in Fig. 3, for higher Ca doping, however, the temperature of the maximum decreases dramatically, and for the sample with $x=0.4$, there only exhibits a small kink in the $M(T)$ curve. From Fig. 3(b), the inverse of $M(T)$ of sample $x=0.4$ shows a downturn deviation from high-temperature linear behavior with decreasing temperature, which indicates that at low temperature the sample $x=0.4$ shows a weak ferromagnetism. The branching of the ZFC and FC data shown in the inset of Fig. 3 approves the ferromagnetism in the sample $x=0.4$. The change of magnetic behavior by Ca doping may arise from following aspects: (1) some holes enter into $CoO_{1+\delta}$ and destruct the effective antiferromagnetic coupling; (2) intermixing of Cu and Co ion induced by Ca doping[10] breaks the Co-O chain; (3) some structure transformation changes the Co coordination. The following results will suggest that the first supposition may be the most possible.

Resistivity as a function of temperature is displayed in Fig. 4 for the annealed samples $x=0.0-0.4$. Substitution of Y by Ca reduces the resistivity fiercely with magnitude change of three orders at room temperature from $x=0.0-0.4$. A metal-insulator transition induced by doping Ca is clearly observed with increasing doping level. In contrast to the large resistivity and insulatorlike behavior in Ca-free Co1212 sample, the resistivity of the sample $x=0.2$ is reduced dramatically by nearly 1000 times at room temperature, and it

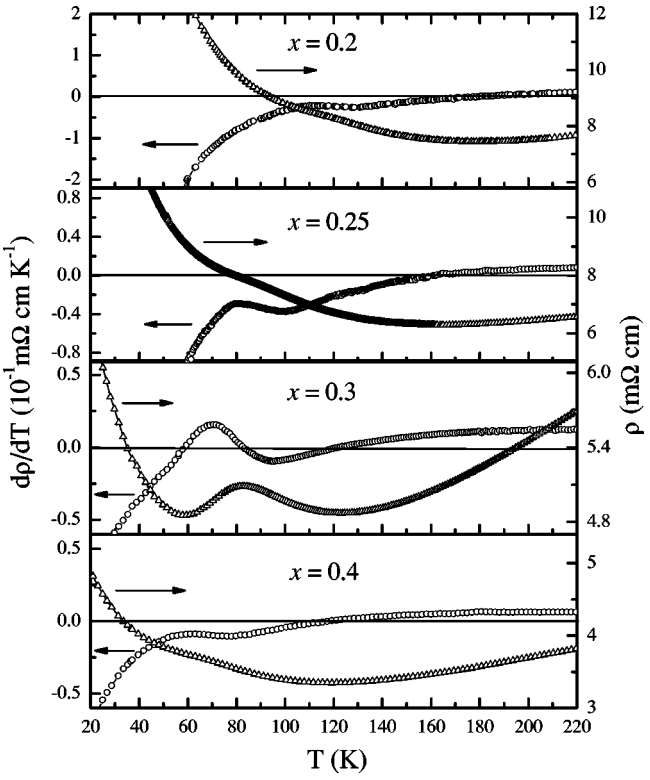

FIG. 5. The resistivity and its derivative as a function of temperature for the samples with $x=0.2$, 0.25, 0.3, 0.4.

exhibits a metallic behavior with a positive slope within a wide temperature region below room temperature. Doping Ca up to $x=0.4$, the resistivity at room temperature is very close to that of the superconducting cuprates. Since the conductive unit in high-T_c cuprates is the CuO_2 plane, a drastic drop of resistivity induced by Ca substitution for the Y ion demonstrates that doped holes enter into the CuO_2 plane indeed. The variation of resistivity with doping is associated with the magnetic results discussed above. However, none of the samples shows SC at the temperature down to 2 K. The reason for the absence of SC has been ascribed to the fact that slight Co ions enter into the CuO_2 plane and destroys its integrality,[10] or that some holes are trapped in the $CoO_{1+\delta}$ charge reservior.[9] It is excluded from the former interpretation since it can be become superconducting by annealing as-synthesized samples in 5 GPa oxygen[9] (this seems to be unable to rearrange the occupational sites). Otherwise, our results seem to demonstrate that the charge reservoir participates in charge transport, that is, there exist holes in the $CoO_{1+\delta}$ layers.

In Fig. 4, there exists a small peak at low temperature for the samples of $x=0.2$, 0.25, 0.3, and 0.4 with a noticeable change in the slope $[d\rho(T)/dT]$. In Fig. 5, the derivative of the resistivity for the four samples $x=0.2$, 0.25, 0.3, 0.4 shows a shallow dip-hump feature. It is found that the temperature at maximum of $M(T)$ corresponds to this dip-hump zone for these four samples. It suggests that the peak observed in resistivity is related to the maximum of the magnetization $M(T)$. In order to find out the correlation between resistivity and magnetization, the curvature $[d^2\rho(T)/dT^2]$ and the $M(T)$ curves are shown in Fig. 6. The temperatures of maximum of $M(T)$ are almost the same as that corresponding to the minimum of $d^2\rho(T)/dT^2$ for the four samples, with the largest difference less than 10 K for the sample $x=0.2$. These results indicate that when Ca content x is as large as 0.2, electrical transport behavior becomes related to magnetic properties closely.

What is the nature of this correlation between charge transport and magnetic behavior? As mentioned previously, the CuO_4 chains participate in the *b*-axis charge transport in Cu1212, and give a slight contribution to the resistivity and lead to a different temperature dependence from that of the *a* axis. In our case, magnetic properties in this system originate from the $CoO_{1+\delta}$ charge reservoir, and the main conducting unit is the CuO_2 plane. Two possible reasons can be considered to interpret the fact that the charge transport is closely related to magnetic properties: (i) the couplings between the itinerant charge carrier in the CuO_2 planes and the localized ordered spin in the $CoO_{1+\delta}$ charge reservoir lead to the correlation; (ii) likely to Cu1212, the charge reservoir participates in charge transport, so that the magnetic transition that occurred in $CoO_{1+\delta}$ influences the charge transport. The behavior exhibited in Co1212 is not the former case because the correlation between magnetic and charge transports is different from that in Ru1212 and Ru1222, in which there exists a ferromagnetic transition in the RuO_2 plane, but no apparent change in resistivity is observed at Curie temperature.[21,22] This assumption is further tested by the magnetotransport data discussed later. In this way, the system contains contributions from two types of conducting layers: $CoO_{1+\delta}$ layers and CuO_2 planes, although the component arising from the charge reservoir layers may be rather little. Therefore, an apparent change in resistivity is observed when a magnetic transition takes place in $CoO_{1+\delta}$, then the dip-hump structure on $d\rho T/dT$ is related to magnetic transition on the charge reservoir layers.

This speculation is confirmed by the magnetotransport data. As shown in Fig. 7, the sample $x=0.3$ exhibits positive magnetoresistance (MR), less than 1% at magnetic field as high as 14 T, while the sample $x=0.4$ shows a negative MR, larger than 14% at 14 T, which seems to be like the behavior in ferromagnetic metal. These contrasting behaviors manifest that the magnetism is transformed from low-dimensional antiforremagnetism in the sample $x=0.3$ to weak ferromagnetism in the sample $x=0.4$, a different MR behavior occurs, and the change in resistivity behavior with Ca doping is closely associated with that in magnetism. Furthermore, the different MR behavior associated with the different magnetic properties located on the $CoO_{1+\delta}$ layers further confirms that the $CoO_{1+\delta}$ charge reservoir participates in charge transport. In Ru-1212 and Ru1222, a maximum negative MR is observed at T_{curie} (ferromagnetic transition temperature).[21,22] This MR behavior has been attributed to the interaction between the Ru moment in RuO_2 planes and itinerant carriers in CuO_2 planes.[21,22] However, the sample $x=0.4$ in Co1212 shows a different MR behavior from Ru1212 and Ru1222. An increase in negative MR with decreasing temperature is observed in Co1212, and the MR in Co1212 is much larger than that in Ru1212 and Ru1222. These differences between Co1212 and Ru1212 (Ru1222) is also an indication for sig-

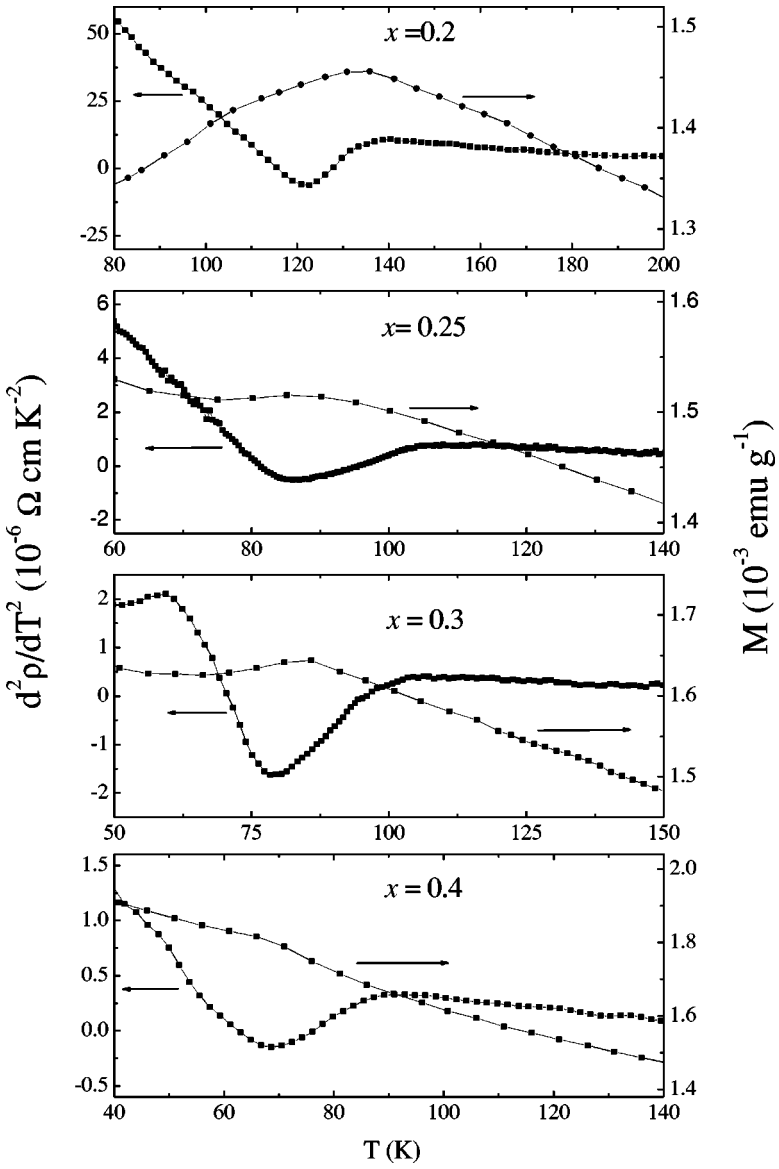

FIG. 6. The temperature dependence of the resistivity curvature ($d^2\rho/d^2T$) and magnetization for the samples with $x=0.2$, 0.25, 0.3, 0.4.

nificant current flowing in $CoO_{1+\delta}$ layers. The Kohler's plot for the samples is shown in the inset of Fig. 7. It should be noted that the MR of the samples with $x=0.3$ and 0.4 does not obey Kohler's rule. This is because below 110 K the charge becomes localized instead of a metal as above 110 K. The MR of the sample $x=0.4$ is proportional to a square of magnetic field, while that of the sample $x=0.3$ shows saturation at high field. In addition, the evolution of the magnetic properties with Ca doping supports a minor charge carrier in $CoO_{1+\delta}$ layers. For the samples with Ca content $x \leqslant 0.2$, the holes induced by Ca substituting for Y are completely introduced into CuO_2 planes, so that the resistivity decreases apparently and the magnetic behavior originated from $CoO_{1+\delta}$ layers does not change with Ca doping. However, further doping Ca leads to a dramatic change in the magnetic behavior and an associated change in resistivity with magnetic behavior. It suggests that the change of magnetic properties is induced by the transfer of the holes into the $CoO_{1+\delta}$ layers when the Ca content $x>0.2$. It should be pointed out that the ferromagnetism occurred in RuO_2 layers does not change with the doping level.

The consideration that holes enter into the $CoO_{1+\delta}$ charge reservoir for the high Ca doping samples is confirmed by further XPS results. The Co $2p$ spectra obtained for the samples $x=0.1$ and 0.4 were shown in Fig. 8. Comparing to the spectrum of the sample $x=0.1$, the binding energy of the two main components, Co $2p_{3/2}$ and $2p_{1/2}$ in the spectrum for the sample $x=0.4$, shift toward higher energy as shown by the solid straight line in the figure. The spectra were analyzed using a peak synthesis program in which a nonlinear background is assumed.[23] For the sample $x=0.1$, the Co$2p$ spectrum shows two main components at about 779.3 and 794.8 eV, which are attributed to Co^{3+} ions.[24] In comparison with the spectrum of the sample $x=0.1$, the two peaks corresponding to the two components Co $2p_{3/2}$ and $2p_{1/2}$ become broad, especially, an apparent doublet is observed for the component Co $2p_{1/2}$. The peaks in the spectrum of $x=0.4$ have to be fitted by two components. By fitting, the doublet positions are determined to be at 797 and 795.3 eV for the Co $2p_{1/2}$, and at 781.2 and 779.8 eV for the Co $2p_{3/2}$, respectively. As pointed out in Ref. 24, the binding energies of 779.8 and 795.3 eV correspond to Co^{3+} ions, while 781.2

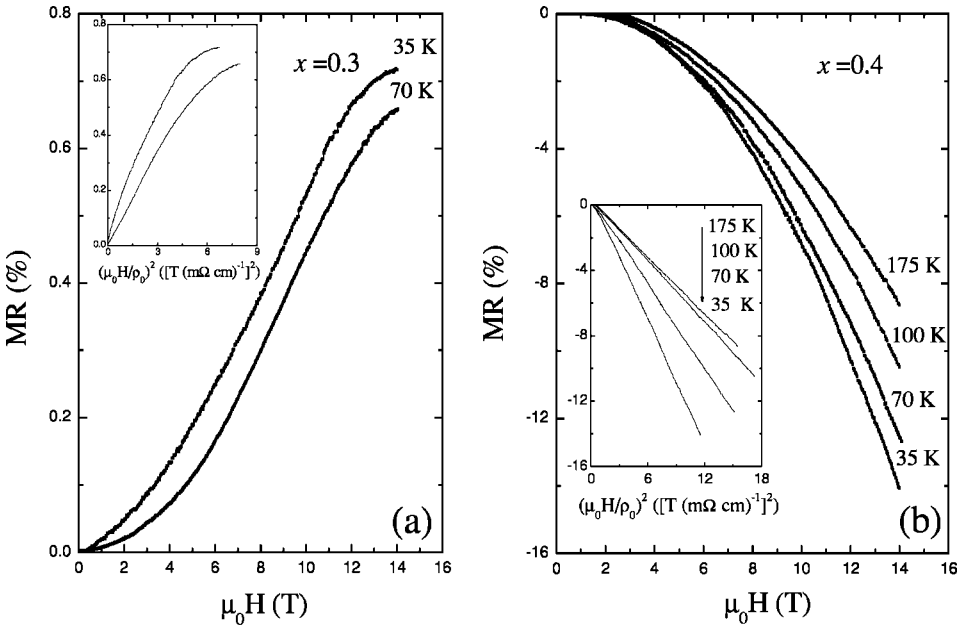

FIG. 7. The plot of magnetoresistance ($MR=[\rho(T,H)-\rho(T,0)]/\rho(T,0)\times 100\%$) vs magnetic field ($\mu_0 H$) for the samples with $x=0.3$, 0.4. Insets: the same data are shown in Kohler's plot.

and 797.0 eV are attributed to Co^{4+} ions. This is evident by the presence of an obvious shoulder on the high-energy side of the Co $2p_{1/2}$ component (marked by the arrow in the figure). These facts clearly show the increase of the valence of Co and confirm the transfer of the holes into the $CoO_{1+\delta}$ layers by increasing the Ca doping level.

It has been reported that CoO_4 tetrahedra in Ca-free Co1212 has a rigid configuration in terms of the oxygen content, and annealing in flowing Ar or O_2 has little effect on oxygen stoichiometry.[16] It is found that no obvious difference in resistivity value or its behavior is observed in AS, 175 atm oxygen annealing, and 195 atm oxygen annealing samples for $x=0.1$, 0.2, 0.25, 0.3, and 0.4 (not shown here). From the analysis on magnetic and transport behavior above, doping of Ca does induce holes into $CoO_{1+\delta}$ although the amount of these holes may be much smaller than that of holes entering into CuO_2 planes for the same Ca doping level. From iodometric titration experiment by Morita *et al.*,[9] the oxygen content almost remains constant, thus holes entering into $CoO_{1+\delta}$ increases the oxidation state of Co. When magnetic ordering occurs in insulating Co^{3+}-O matrix, the magnetism occurred in $CoO_{1+\delta}$ layers has a very weak effect on the charge transport. The magnetic effect on resistivity originates from the coupling between the itinerant carrier and the local ordered spin in the $CoO_{1+\delta}$ layers. When hole is doped into $CoO_{1+\delta}$ layers, a ferromagnetic metal (FM) cluster containing Co^{4+} ions may reduce the resistivity apparently, especially for the sample $x=0.4$ in which weak ferromagnetism shows up. This picture has been used to interpret the noticeable change of the slope in $\rho(T)$ of $La_{0.85}Sr_{0.15}CoO_3$ and $La_{0.75}Sr_{0.25}CoO_3$ films.[25] In fact, in the inset of Fig. 3, the ZFC and FC magnetization curves of the samples $x=0.25$ and 0.4 start branching around the temperatures corresponding to the maximum of magnetization, indicative of some ferromagnetic component. However, as reported in Ref. 11, for the Ca-free sample no ZFC and FC branching are observed. These results suggest that the Ca-free sample contains no ferromagnetic component, while as the Ca doping level is higher than 0.2, the system becomes a intermixture of a antiferromagnetic and ferromagnetic component. The temperature dependence of the magnetization for the sample $x=0.2$, 0.25, and 0.3 exhibits antiferromagnetism, indicating that in these samples the ferromagnetic component is rather small. While for the sample $x=0.4$, it exhibits weak ferromagnetism, indicating that in this sample the ferromagnetic component is already preponderant. This may interpret the large MR in the sample $x=0.4$, while rather the small MR in the sample $x=0.3$. It is not clear whether the partly intermixing between Co and Cu has any effect on the resistivity. More microscopic studies on the electronic state of Co ions(Co^{3+} or Co^{4+}) in the charge reservoir is needed to explain this phenomena completely.

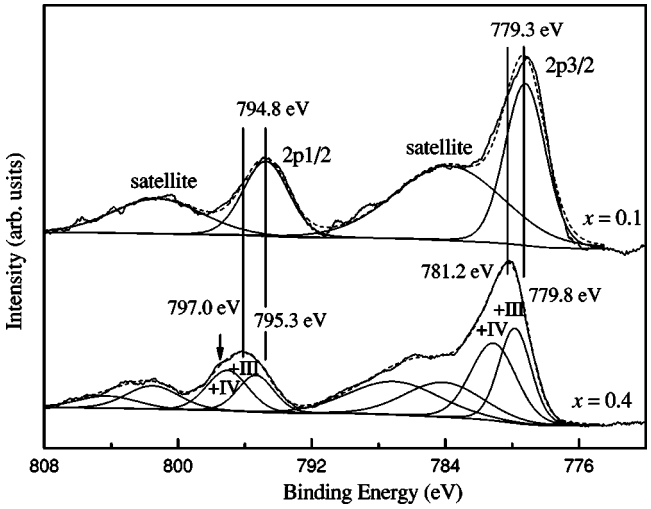

FIG. 8. The Co2*p* XPS spectra for the sample $x=0.1$ and 0.4.

IV. CONCLUSION

We have synthesized polycrystalline $CoSr_2Y_{1-x}Ca_xCu_2O_{7+\delta}$($x=0.0-0.4$), and investigated their

magnetic and transport properties. In the sample $x=0.0-0.2$, magnetization shows a broad maximum at low temperature (almost the same temperature), indicative of low-dimensional antiferromagnetic nature originated from $CoO_{1+\delta}$ layers. The temperature of such a maximum for the sample $x=0.3$ drops dramatically, and for the sample with $x=0.4$ a weak ferromagnetism shows up. Ca doping reduces resistivity quickly. $d\rho(T)/dT$ shows a dip-hump feature at low temperature for the samples with $x=0.2-0.4$, which is ascribed to a contribution of holes in $CoO_{1+\delta}$ charge reservoir and magnetic transition within the layers. The speculation is confirmed by the fact that a small positive MR exhibits in the sample $x=0.3$, while the large negative MR in the $x=0.4$ sample.

ACKNOWLEDGMENTS

This work is supported by the grant from the Nature Science Foundation of China and by the Ministry of Science and Technology of China (Grant No. NKBRSF-G1999064601), and the Knowledge Innovation Project of Chinese Academy of Sciences.

*Electronic address: chenxh@ustc.edu.cn

[1] J. M. Tarascon and B. G. Bagley, in *Chemistry of High Temperature Superconductors*, edited by A. Vanderaha (Noyes, New York 1993), pp. 310, and references therein.
[2] R. Gagnon, C. Lupien, and L. Taillefer, Phys. Rev. B **50**, 3458 (1994).
[3] S. A. Sunshine, L. F. Schneemeyer, T. Siegrist, D. C. Douglass, J. V. Waszczak, R. J. Cava, E. M. Gyorgy, and D. W. Murphy, Chem. Mater. **1**, 331 (1989).
[4] G. Roth, P. Adelmann, G. Heger, R. Knitter, and T. Wolf, J. Phys. I **1**, 721 (1991).
[5] M. Isobe, Y. Mutsui, and Takayama-Muromachi, Physica C **222**, 310 (1994).
[6] L. Bauernfeind, W. Widder, and H. F. Braun, Physica C **254**, 151 (1995).
[7] J. Shimoyama, K. Otzschi, T. Hinouchi, and K. Kishio, Physica C **341**, 563 (2000).
[8] S. Adachi, K. Kubo, S. Takano, and H. Yamauchi, Physica C **191**, 174 (1992).
[9] Y. Morita, H. Yamauchi, and M. Karppinen, Solid State Commun. **127**, 493 (2003).
[10] Q. Huang, R. J. Cava, A. Santoro, J. J. Krajewski, and W. F. Peck, Physica C **193**, 196 (1992).
[11] V. P. S. Awana, S. K. Malik, W. B. Yelon, M. Karppinen, and H. Yanauchi, Physica C **378**, 155 (2002).
[12] V. P. S. Awana, E. Takayama-Muromachi, S. K. Malik, W. B. Yelon, M. Karppinen, H. Yamauchi, and V. V. Krishinamuthy, J. Appl. Phys. **93**, 8221 (2003); also see cond-mat/0209605 (unpublished).
[13] J. Ramirez-Castellanos, Y. Matsui, M. Isobe, and E. Takayama-Muromachi, J. Solid State Chem. **133**, 434 (1997).
[14] P. Bordet, F. Licci, C. Bougerol-Chaillout, and M. Marezio, J. Solid State Chem. **149**, 256 (2000).
[15] T. Nagi, V. P. S. Awana, E. Takayama-Muromachi, A. Yamazaki, M. Karppinen, H. Yamauchi, S. K. Malik, W. B. Yelon, and Y. Matsui, J. Solid State Chem. **176**, 213 (2003).
[16] M. Karppinen, V. P. S. Awana, Y. Morita, and H. Yamauchi, Physica C **392**, 82 (2003).
[17] M. Matoba, T. Takeuchi, S. Okada, Y. Kamihara, M. Itoh, K. Ohoyama, and Y. Yamaguchi, Physica B **312**, 630 (2202).
[18] Y. Kamihara, M. Matoba, T. Kyomen, and M. Itoh, J. Appl. Phys. **91**, 8864 (2002).
[19] C. S. Knee, A. A. Zhukov, and M. T. Weller, Chem. Mater. **14**, 4249 (2002).
[20] R. Navarro, J. J. Smit, L. J. de Jongh, W. J. Crama, and D. J. W. Ijdo, Physica B & C **83**, 97 (1976).
[21] J. E. McCrone, J. R. Cooper, and J. L. Tallon, J. Low Temp. Phys. **117**, 1199 (1999).
[22] X. H. Chen, Z. Sun, K. Q. Wang, S. Y. Li, Y. M. Xiong, M. Yu, and L. Z. Cao, Phys. Rev. B **63**, 064506 (2001).
[23] D. A. Shirley, Phys. Rev. B **5**, 4709 (1972).
[24] J. C. Dupin, D. Gonbeau, H. Benqlilou-Moudden, P. Vinatier, and A. Levasseur, Thin Solid Films **384**, 23 (2001).
[25] G. Prokhorov, G. G. Kaminsky, I. I. Kravchenko, and Y. P. Lee, Physica B **324**, 205 (2002).